



Numerical analysis of a barge collision with bridge pier by using finite element method

Kazi Naimul Hoque^{1,*}, Sabrina Salam¹, Mst. Zebun Nahar Eti Moni¹

ARTICLE INFO

Article history:

Received 27 Nov 2023;
in revised from 5 Jan 2024;
accepted 21 Jan 2024.

Keywords:

Barge collision, bridge pier, impact stress, kinetic energy, pier displacement, finite element analysis.

© SEECMAR | All rights reserved

ABSTRACT

This study investigates the structural response of bridge piers to collisions with vessels, focusing on factors such as impact stress, pier displacement, and kinetic energy. Using finite element analysis (FEA) simulations, the study considers various barge velocities and pier material properties. The results show that at lower impact velocities (up to 2 knots), the pier undergoes elastic deformation, while at higher velocities, plastic deformation and potential collapse occur. The material's yield strength is crucial, and high tensile steel may be necessary for velocities exceeding 2 knots. The study emphasizes the importance of accurate modeling and considers alternatives for enhancing pier resilience, contributing to the development of safer maritime structures.

1. Introduction.

The examination of the response of structures to various impact loads using analytical methods and the exploration of finite element analysis are central themes in the study conducted by Woelkea et al. [1]. The study presents a brief overview of analytical methods used to determine the loads and energies associated with ship impact. A linear relationship between the volume of deformed steel and the energy dissipated in the deformation process is established. Additionally, a discussion on a set of empirical expressions for calculating bow collision forces, maximum penetration, and impact duration is included. Another study, conducted by Hu et al. [2], focused on the finite element analysis of the nonlinear collision between a 300k DWT VLCC and a bridge pier. The study accurately simulates the strongly nonlinear process of ship-bridge collision by considering the bridge pier as a rigid body and accounting for the surrounding flow. The analysis includes examining the time history curve of impact force, energy absorption, and damage condition. A comparison is then made between the results obtained from given standards and empirical formulae and those

from finite element simulation. The findings highlight the complexity of the collision as a nonlinear dynamic process with significant energy exchange in a short time.

The work conducted by PINTO et al. presents a study on a flexible protection system for a bridge-pier model, where the barge was modeled nonlinearly [3]. The protection structure was derived through a separate nonlinear pushover analysis, represented by its equivalent load deflection curve and mass. The methodology employed to assess the energy absorption capacity of the protection structure involved the development of a nonlinear numerical model. The study simulated and examined a pier made of rigid concrete material using a numerical approach, and the obtained results were compared with previous findings [4]. In 2011, Lin conducted a study, providing a comprehensive investigation based on trials [5]. However, the experimental study reported no structural damage, potentially attributed to the relatively small energy of the conducted collision.

Zhang et al. develops semi-analytical methods for analyzing plate crushing and ship bow damage in head-on collisions [6]. The study compiles and compares existing experimental and theoretical research on the crushing analysis of plated structures. Simple formulae are derived to determine the crushing force, force-deformation curve, and damage extent of a ship

¹Bangladesh University of Engineering and Technology.

*Corresponding author: Kazi Naimul Hoque. E-mail Address: kazi-naim@name.buet.ac.bd.

bow for longitudinally stiffened oil tankers and bulk carriers with a length of 150 meters and above. These formulae are expressed in terms of ship principal particulars. Kameshwar and Padgett investigates the barge impact performance of bridge piers, considering various design parameters and the free length of the pile, which may be due to design or scour [7]. The study includes a preliminary analysis to evaluate the post-collision safety of bridges under traffic loads. Metamodels are developed to estimate force demands and fragility for bridge piers subjected to barge impact, aiding in the design and management of bridges with diverse design and geometric parameters. Non-linear dynamic analysis is performed to assess maximum shear force, moment, shear strain, and curvature in the columns. After the dynamic analysis, vertical load analysis is conducted to determine the post-collision stability of bridges under vehicular loads. The models developed in this study are applied to a case study bridge, illustrating the variation in demands and fragility as bridge parameters, free pile length (scour depth), and collision conditions are altered.

In this research, a study is conducted to investigate and analyze the behavior, impact forces, and structural responses associated with collisions between vessels and bridge piers. The study aims to find out the following structural behaviors:

- i. To determine impact stress with respect to time in case of a barge pier collision.
- ii. To investigate pier displacement corresponding to different barge velocities.
- iii. To evaluate the progression of impact energy considering different barge velocities.

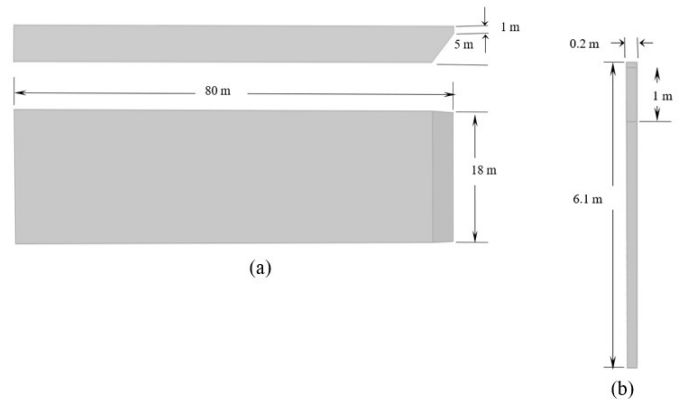
This investigation is carried out with the assumption that the pier material is high carbon steel with a yield strength of 585 MPa. Opting for higher-grade steels, such as high tensile steel, could render the dynamic response, endurance, and material behavior more vulnerable to more severe collision scenarios. Through this study, the aim is to propose improved design criteria and material selection, especially applicable to heavier bridge piers.

2. Model Geometry.

2.1. Modeling the barge and the pier.

In this study, a steel barge and pier are modelled using ABAQUS software. The barge dimensions are 80m x 18m x 5m with a head log portion which directly collides with the pier. The head log has a rectangular cross section with a height of 1m. The deadweight of the barge is taken as 1723 tons. For modelling the steel pier, dimensions from real steel piers were adopted with regards to specifications of Southern Forest Products Association, United States. The pier structure has a square cross section of 0.2m x 0.2m and length is 6.1m. During analysis, the barge collides with the pier with its head log portion, that has a height of 1m. Since the width of the pier is 0.2m, the area under impact load becomes 0.2m x 1m or, 0.2m². The schematic diagram of the barge and pier is shown in Figure 1.

Figure 1: Schematic diagram of the (a) barge, and (b) pier.



Source: Authors.

The properties of the steel for the pier are shown in Table 1 [4].

Table 1: Material properties of steel pier.

Material properties	Magnitude
Mass density	7865 kg/m ³
Young's modulus	207 GPa
Yield strength	505 MPa
Poisson's ratio	0.27

Source: Authors.

2.2. Assigning loads on the pier.

Two types of loads are considered in the analysis; a gravity load on the top of the pier with regard to the weight of the walkway of bridge, taken as 1 ton; and the impact loads for corresponding barge velocities.

Both loads are assigned as pressure force. So, the pressure force due to gravity is calculated as:

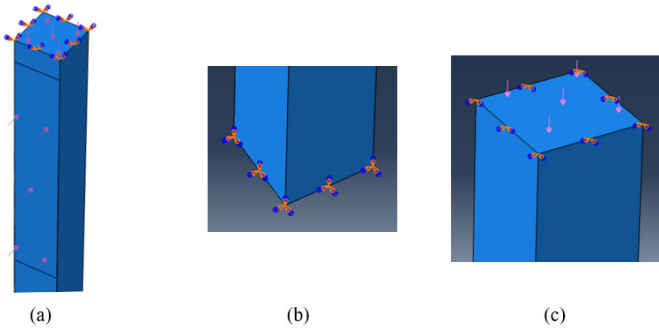
$$\begin{aligned}
 1 \text{ ton} &= 1000 \text{ Kg} \\
 &= 1000 \times 9.8 \text{ N} \\
 &= (1000 \times 9.8) \text{ N} / (0.2 \times 0.2) \text{ m}^2 \\
 &= 245,000 \text{ Pa} \\
 &= 245 \text{ MPa}
 \end{aligned}$$

Loading conditions are depicted in Figure 2, with assigned load values for each simulation in the same direction, maintaining a consistent angle of impact.

2.3. Boundary conditions on the pier.

The lower surface of the pier is supported by the ground, implying no movement along any axis. Consequently, the bottom surface of the pier was constrained in all three axes, resembling an 'encastre' condition in the software. In ABAQUS software, the 'encastre' condition is defined as fully built-in (degrees of freedom 1,2,3,4,5,6 = 0). However, the top surface is solely supported by the bridge, allowing the pier to deform along the z-axis while restricting movement along the x and y axes. Thus, the boundary conditions are specified as x and y restricted and z unrestricted.

Figure 2: (a) Loads assigned on the pier, (b) boundary condition at the bottom surface of the pier, x, y and z axis restricted, and (c) boundary condition at the top surface of the pier, x and y axis restricted.



Source: Authors.

3. Basic Formulations.

In accordance with AASHTO specifications [8], the impact force was computed using the subsequent formula:

$$P_{bow} = 0.12V_0 \sqrt{DWT} \quad (1)$$

where,

P_{bow} = maximum bow collision load [MN]

V_0 = initial ship velocity [m/s]

DWT = deadweight of the vessel in metric tons

This equation was employed to input impact loads for various velocities and deadweights in the simulations performed in this research. According to this equation, the load imposed by the bow is directly proportional to the barge velocity, leading to a stress input that is also proportionate to the impact velocity. Nevertheless, in the simulation conducted with ABAQUS software, an algorithm for determining von-Mises stress at the structure's most vulnerable region was also examined [9].

In generating output for von-Mises stress, it is important to recognize that von-Mises stress is a geometric combination of all stresses (normal stress in three directions and all three shear stresses) acting at a specific location. If the von-Mises stress at a particular location surpasses the yield strength, the material yields at that point. If the von-Mises stress exceeds the ultimate strength, the material ruptures at that location. The failure criterion asserts that the von-Mises stress σ_{mises} should be lower than the yield stress (σ_y) of the material. In its inequality form, the criterion can be expressed as:

$$\sigma_{mises} \leq \sigma_y$$

The von-Mises stress σ_{mises} is given by,

$$\sigma_{mises} = \sqrt{I_1^2 - 3I_2} \quad (2)$$

where I_1 and I_2 are given by,

$$I_1 = \sigma_x + \sigma_y + \sigma_z \quad (3)$$

$$I_2 = \sigma_x\sigma_y + \sigma_y\sigma_z + \sigma_z\sigma_x - \tau_{yz}^2 - \tau_{xz}^2 - \tau_{xy}^2 \quad (4)$$

4. Results and Discussion.

4.1. Von-Mises stress analysis.

The von-Mises stress against seed size for different barge velocities are shown in Table 2 to Table 4.

Table 2: Maximum stress values for a barge velocity of 1 knot:

Table 2: Maximum stress values for a barge velocity of 1 knot.

Seed size (m)	von-Mises stress (GPa)
0.055	0.622
0.05	0.573
0.04	0.541
0.03	0.509
0.02	0.477

Source: Authors.

The von-Mises stresses resulting from the barge impact on the pier at a velocity of 1 knot have been consolidated in Table 2. For the largest considered seed size, namely 0.055, the induced stress was 0.622 GPa. Upon reducing the seed size to 0.05, the stress experienced a decline to 0.573 GPa. Subsequently, with a seed size of 0.04, the maximum stress reached 0.541 GPa. Further reductions in seed size to 0.03 and 0.02 led to stress values of 0.509 GPa and 0.477 GPa, respectively. It is noteworthy that the yield strength of high-strength steel is 0.505 GPa. Consequently, the stresses generated for seed sizes of 0.05 and 0.055 surpass the yield strength limit of the pier material, entering its permanent deformation range.

The generated von-Mises stress for a barge velocity of 2 knots exhibited a similar trend with varying seed sizes, as outlined in Table 3. The stress reached its maximum value of 1.29 GPa with a seed size of 0.055, followed by a subsequent decrease to 1.03 GPa for a smaller seed size of 0.05. A further reduction in stress was observed with a seed size of 0.04. The smallest stresses were recorded for seed sizes of 0.03 and 0.02, measuring 0.68 GPa and 0.54 GPa, respectively. Therefore, for a barge velocity of 2 knots, elevated stresses were noted when using seed sizes of 0.03 and above, surpassing the yield strength of the pier. Consequently, the pier may undergo plastic deformation if subjected to a barge impact at a velocity of 2 knots.

Table 3: Maximum stress values for a barge velocity of 2 knots.

Seed size (m)	von-Mises stress (GPa)
0.055	1.29
0.05	1.03
0.04	0.89
0.03	0.68
0.02	0.54

Source: Authors.

Table 4: Maximum stress values for a barge velocity of 3 knots.

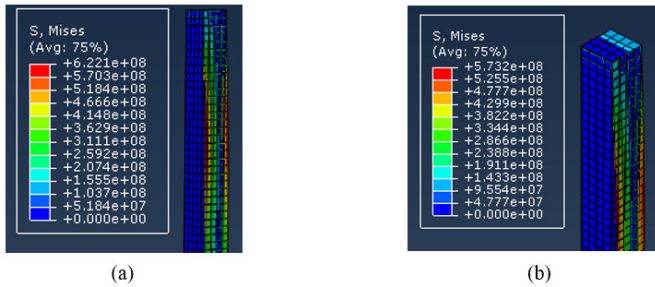
Seed size (m)	von-Mises stress (GPa)
0.055	3.03
0.05	2.09
0.04	1.89
0.03	1.74
0.02	1.66

Source: Authors.

When considering a velocity of 3 knots, the von-Mises stresses exhibited an increasing trend with growing seed sizes, as detailed in Table 4. Starting with a seed size of 0.055, the pier experienced a peak stress of 3.03 GPa. Subsequently, a notable decrease was observed for a smaller seed size of 0.05, registering at 2.09 GPa. Another decrease in stress was noted with a seed size of 0.04. Finally, the smallest seed sizes, 0.03 and 0.02, yielded the minimum stresses at 1.74 GPa and 1.66 GPa, respectively. With the increase in barge velocity to 3 knots, even higher stresses were generated. Given that high strength steel has an ultimate tensile strength of 1.20 GPa, it is evident from the table that all von-Mises stresses exceed this value. Consequently, the pier is prone to cracking, crushing, or collapsing if impacted by a 1723 DWT barge at a velocity of 3 knots.

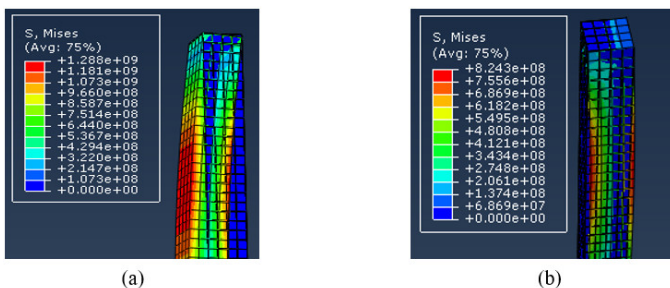
The analysis of von-Mises stress against seed size for different barge velocities are shown in Figure 3 to Figure 5.

Figure 3: Von-Misses stress for (a) seed size 0.055m, and (b) seed size 0.05m, considering 1 knot barge velocity.



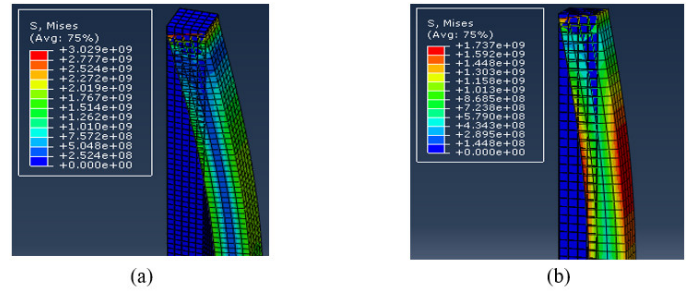
Source: Authors.

Figure 4: Von-Misses stress for (a) seed size 0.055m, and (b) seed size 0.04m considering 2 knots barge velocity.



Source: Authors.

Figure 5: Von-Misses stress for (a) seed size 0.055m, and (b) seed size 0.03m considering 3 knots barge velocity.



Source: Authors.

4.2. Pier displacement analysis.

The displacement against seed size for different barge velocities are shown in Table 5 to Table 7.

Table 5: Maximum displacement for a barge velocity of 1 knot.

Seed size (m)	Displacement (mm)
0.055	65.90
0.05	58.15
0.04	34.42
0.03	17.71
0.02	10.24

Source: Authors.

Table 5 illustrates pier displacements corresponding to various seed sizes obtained from the simulations. When a seed size of 0.055 was employed, the pier exhibited a peak displacement of 65.90 mm. Subsequently, with a seed size of 0.05, the displacement reduced to 58.15 mm. Opting for a smaller seed size of 0.04 resulted in a displacement of 34.42 mm. Further reductions in seed size to 0.03 and 0.02 yielded displacements of 17.71 mm and 10.24 mm, respectively. Hence, the pier displacement demonstrated a consistent trend, where decreasing seed size led to smaller displacement values.

Table 6: Maximum displacement for a barge velocity of 2 knots.

Seed size (m)	Displacement (mm)
0.055	70.21
0.05	63.28
0.04	51.02
0.03	39.55
0.02	23.50

Source: Authors.

Table 6 presents pier displacements corresponding to a barge velocity of 2 knots for various seed sizes. Using a seed size of 0.055, the pier exhibited a peak displacement of 70.21 mm. Subsequently, with a seed size of 0.05, the displacement reduced to 63.28 mm. Opting for a smaller seed size of 0.04

resulted in a displacement of 51.02 mm. Further reductions in seed size to 0.03 and 0.02 yielded displacements of 39.55 mm and 23.50 mm, respectively.

Table 7: Maximum displacement for a barge velocity of 3 knots.

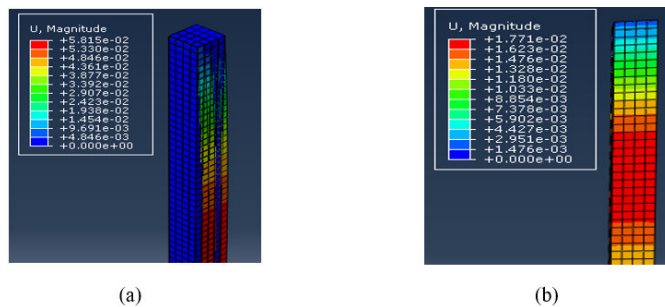
Seed size (m)	Displacement (mm)
0.055	165.6
0.05	133.8
0.04	111.8
0.03	64.48
0.02	58.37

Source: Authors.

Table 7 displays pier displacements corresponding to a barge velocity of 3 knots for various seed sizes. Using the largest seed size of 0.055, the displacement measured 165.6 mm. With a seed size of 0.05, the pier exhibited a peak displacement of 133.8 mm. Opting for a smaller element seed size of 0.04 resulted in a displacement of 111.8 mm. Further reducing the element seed size to 0.03 led to a pier displacement of 64.48 mm. The smallest seed size of 0.02 yielded a displacement of 58.37 mm. It is noteworthy that the displacements for seed sizes 0.03 and 0.02 are quite close, indicating mesh convergence.

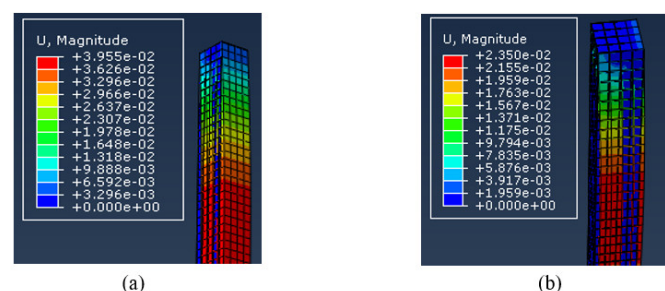
The analysis of pier displacement against seed size for different barge velocities is shown in Figure 6 to Figure 8.

Figure 6: Displacement for (a) seed size 0.05m, and (b) seed size 0.03m with 1 knot barge velocity.



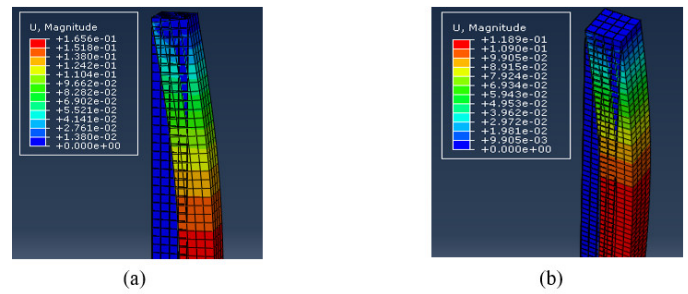
Source: Authors.

Figure 7: Displacement for (a) seed size 0.03m, and (b) seed size 0.02m with 2 knots barge velocity.



Source: Authors.

Figure 8: Displacement for (a) seed size 0.055m, and (b) seed size 0.05m with 3 knots barge velocity.



Source: Authors.

4.3. Kinetic Energy Analysis.

From the first two plots in Figure 9, it is evident that the impact energy vs. time curve exhibits a broader amplitude at a higher velocity of 2 knots compared to 1 knot. This indicates that the impact energy fluctuates on a larger scale when the barge velocity is increased. Similarly, when comparing impact energy for different seed sizes while maintaining a velocity of 3 knots as shown in Figure 10, a wider amplitude has been observed for the smaller seed size.

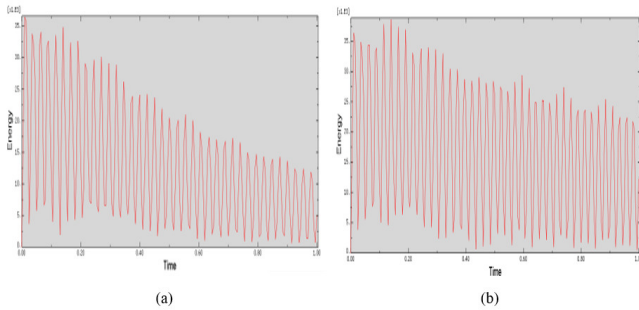
A consistent pattern observed in all the plots is the gradual decay of energy over time. This occurs because the maximum energy transfer takes place at the moment of collision between the barge and the pier. As time progresses, the energy is dispersed into the surrounding water, resulting in a reduction in the associated kinetic energy. To further confirm the diminishing trend and decrease in the amplitude of the energy curves, findings were examined from the research conducted by Sha and Hao [4]. In their study, the researcher plotted the impact force vs. time duration curve using LS Dyna, revealing a maximum impact force at the time of collision, with the associated impact energy dissipating as time advances [4]. The plotted impact forces reached a maximum value at a velocity of 4.11 m/s and gradually declined, reaching the minimum peak impact force for a velocity of 0.51 m/s.

Figure 9 and Figure 10 clearly show that the impact force reaches its peak immediately after the collision. Evidently, the kinetic energy also peaks during the same time duration. As time progresses, the impact energy diminishes, leading to a sharp downward curve with a reduction in amplitude. A similar pattern was identified in this study, where the curves exhibited both trends for all the simulations. Consequently, the results are corroborated and validated.

4.4. Maximum stress for different barge velocities.

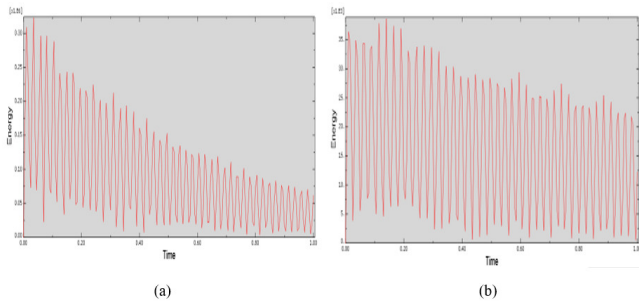
To determine the maximum stress generated in collisions at each velocity condition, peak values from analysis results were gathered and plotted against corresponding seed sizes. For example, the von-Mises stress generated as the pier was struck by the barge with a velocity of 1 knot. From this analysis, the maximum stress of 0.477 GPa was selected to plot against a mesh size of 0.02m in the graph.

Figure 9: Kinetic energy with time using (a) seed size 0.055m for 1Knot barge velocity, and (b) seed size 0.04m for 2 knots barge velocity.



Source: Authors.

Figure 10: Kinetic energy with time using (a) seed size 0.055m, and (b) seed size 0.04m for 3 knots barge velocity.



Source: Authors.

For each barge velocity, maximum stress values were extracted for mesh sizes of 0.055m, 0.05m, 0.04m, 0.03m, and 0.02m, and these values were plotted in a graph. More precise stress values were observed for smaller mesh sizes, resulting in a flattening of the graph in the smaller mesh region. The accuracy of the results was thus verified through the mesh convergence of the plots.

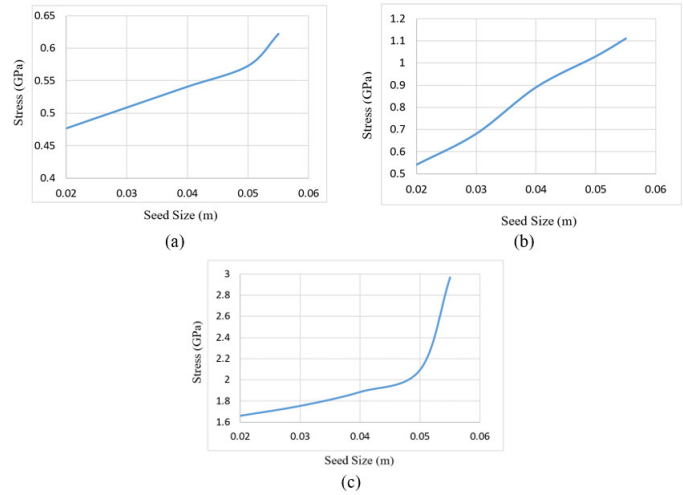
As evident from the result from Table 2 to Table 4, stresses remained within the yield strength limit of steel when the barge velocity was up to 2 knots. However, as the velocity increased to 3 knots, the stress reached 0.54 GPa, surpassing the yield strength of steel.

To validate the trends observed in the analysis, research work conducted by Liu et al. [10] was considered. In this study, the authors designed optimal manufacturing structures and investigated patterns for von-Mises stress and displacement under dynamic loading conditions [10].

In this research, the researcher considered the smallest inner side with 1.3 mm and the maximum inner side with 5.4 mm. The maximum von-Mises stress for the smallest seed size was 42.23 MPa, and the maximum von-Mises stress for the maximum seed size was 160.3 MPa. For the smallest seed size, the maximum displacement was 0.167 mm, and for the largest seed size, the maximum displacement was 0.508 mm.

The results indicate that as the number of seed size increases, the inner wall width (mesh size) decreases, leading to a reduc-

Figure 11: Maximum stress vs. seed size in case of steel piers under a fully loaded barge with an impact velocity of (a) 1 knot, (b) 2 knots, and (c) 3 knots.



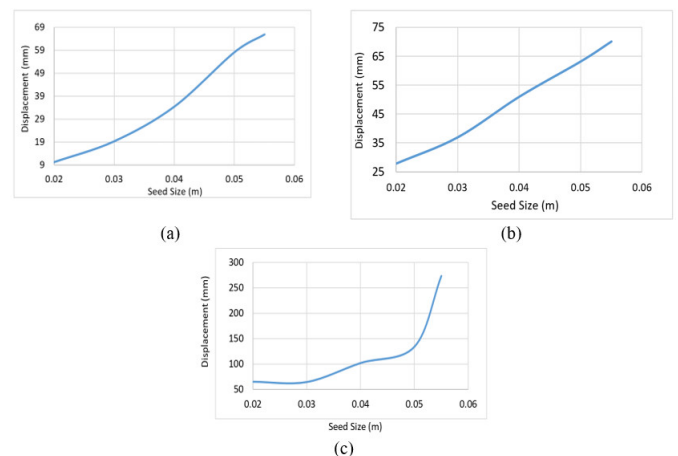
Source: Authors.

tion in the maximum von-Mises stress of the structure. Similarly, the maximum displacements are minimized for smaller seed sizes. This suggests that, in their study, a graph would exhibit a downward pattern as well [10]. In other words, a smaller mesh size results in more accurate outcomes, i.e., lower stress and displacement, confirming the simulation results obtained in this study.

4.5. Maximum displacement for different barge velocities.

Likewise, peak displacement values were extracted for mesh sizes of 0.055m, 0.05m, 0.04m, 0.03m, and 0.02m. These values were then plotted in graphs corresponding to each analyzed velocity condition, as illustrated in Figure 12.

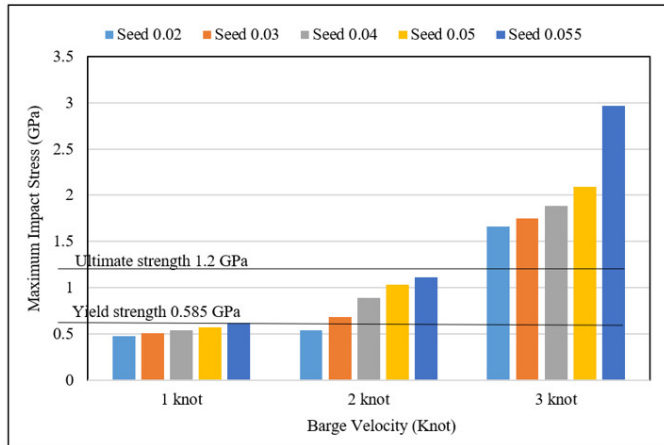
Figure 12: Displacement vs. seed size for a barge velocity of (a) 1 knot, (b) 2 knots, and (c) 3 knots.



Source: Authors.

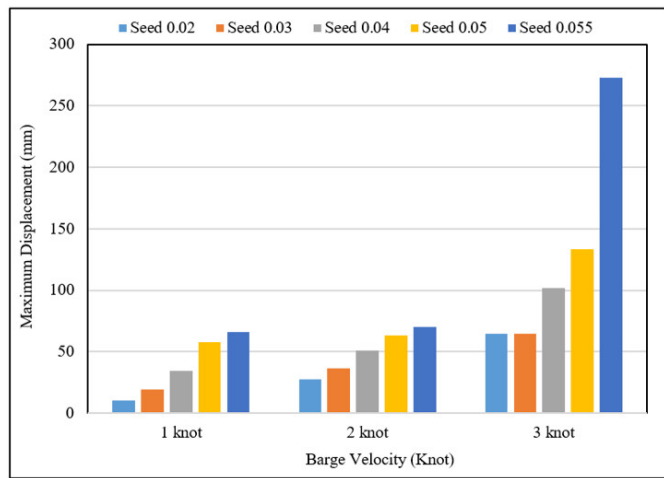
4.6. Comparative Analysis.

Figure 13: Maximum impact stress plotted against seed size for different barge velocities.



Source: Authors.

Figure 14: Maximum displacement plotted against seed size for different barge velocities.

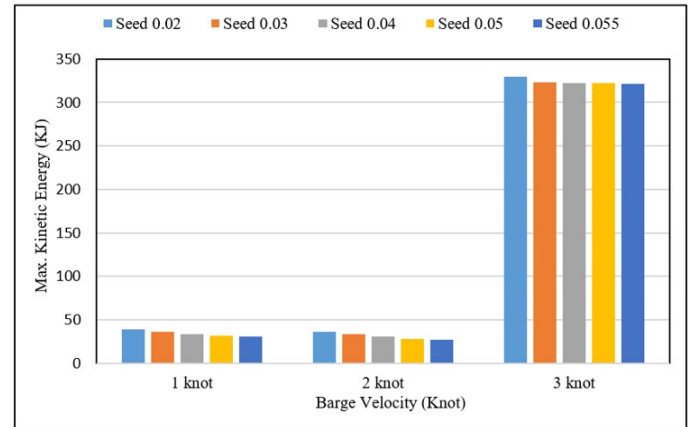


Source: Authors.

Figure 13 provides a clear indication that a steel pier, given its specified weight and dimensions, will not undergo permanent deformation in the event of a collision with a barge traveling at a maximum velocity of 2 knots. At a barge velocity of 1 knot, the maximum impact stress remains within the yield strength of the chosen material, ensuring no permanent deformation. However, when subjected to higher barge velocities exceeding 2 knots, the pier is prone to collapse due to the maximum impact stress surpassing the ultimate strength threshold of the material.

In Figure 14, the plotted data for maximum displacements reveals a discernible trend. As the seed size decreases, indicating a finer mesh resolution, the displacement values exhibit a reduction. Concurrently, as the velocity of the barge increases,

Figure 15: Maximum kinetic energy plotted against seed size for different barge velocities.



Source: Authors.

the corresponding displacement values tend to rise. This observation implies that the likelihood of the pier surviving a collision with the barge diminishes as the barge velocity increases. The inverse relationship between seed size and displacement, coupled with the direct correlation between barge velocity and displacement, underscores the importance of finer mesh resolution for accurate assessments of pier survivability under varying collision scenarios.

In Figure 15, the depicted trend illustrates the maximum kinetic energy across various barge velocities. Notably, a reduction in seed size corresponds to a decrease in the maximum kinetic energy, while an increase in barge velocity is associated with an elevation in kinetic energy values. Remarkably, at 1 and 2 knots barge velocities, the maximum kinetic energy is lower compared to the 3 knots barge velocity scenario. This observation is significant, as higher kinetic energy levels are indicative of increased potential for deformation in the pier structure. Thus, the trend underscores the critical role of kinetic energy considerations in assessing the extent of pier deformation resulting from collisions at varying velocities.

Conclusions.

This study delved into the structural response of a pier in diverse collision scenarios involving barges. Employing FEA, a comprehensive examination of parameters such as material properties, geometry, boundary conditions, and impact velocities was conducted. The study focused on a steel pier model to investigate the impact of pier material and barge velocity on stress, displacement, and associated energy during collisions. The results underscore the significance of considering bridge pier material properties in understanding barge-pier collision responses. Findings reveal that at lower impact velocities, the pier experiences elastic deformation, recovering its position post-collision. However, at higher impact velocities, plastic deformation and complete damage are observed.

The study limited the barge velocity to 3 knots, acknowledging that practical scenarios might involve higher velocities

during collision, resulting in greater impact force, stress, kinetic energy, and displacement. Consequently, the examined high carbon steel piers, given their weight and dimensions, can only withstand barge collisions with a maximum velocity of 2 knots. Beyond this threshold, the pier exhibits nonlinear deformation, and the likelihood of collapse increases with escalating barge velocity. For situations where the pier faces potential collisions exceeding 2 knots, alternative materials or pier dimensions should be considered.

Two primary alternatives emerged from the study. First, designing the pier with larger dimensions can prevent stress from surpassing the yield strength of the steel. The ultimate alternative involves designing the pier with a material of higher strength, such as high tensile steel, where the yield strength exceeds the maximum impact stress in worst-case collision scenarios. This study emphasizes the importance of design considerations using FEM as a tool for enhanced structural consciousness.

The simulations provided precise insights into dynamic behavior, deformation patterns, and stress distribution within structures, crucial for optimizing barge and pier design, enhancing safety, and ensuring durability. The study underscored the significance of considering impact velocity, material properties, and boundary conditions in assessing collision response, influencing structural behavior, and necessitating effective mitigation strategies. Additionally, accurate modeling and validation of FEA simulations were emphasized through comparison with theoretical material behavior, ensuring reliability. In conclusion, the study's findings contribute to safer and more resilient structures in maritime transportation, serving as a foundation for future research to refine modeling techniques, incorporate additional factors, and explore dynamic behaviors in various maritime structures under collision scenarios.

Acknowledgements.

The authors extend heartfelt thanks to all those who have offered valuable support at different stages of this research work, both directly and indirectly. Special recognition is given to the UGC HEQEP Sub Project "Strengthening the Research Capa-

bilities and Experimental Facilities in the Field of Marine Structure" (CP#3131), which has played a crucial role in improving the simulation lab facilities. Additionally, gratitude is expressed to the "Basic Research Grant" for providing financial support to enhance the research endeavors.

References.

- [1] Pawel Woelke, Najib Abboud, Darren Tennant, Eric Hansen and Chad Mearthur, "Ship impact study: Analytical approaches and finite element modeling" (2011).
- [2] Zhen-Biao Hu, Ke-Cheng Zhang, Yao-Hua Fu and Yun-Long Jin, "Finite element analysis of the nonlinear collision between 300k DWT VLCC and bridge pier", International Collaboration in Lifeline Earthquake Engineering (2016).
- [3] Frederico PINTO, F. Jose LUPERI, Carlos A. PRATO, "Design of energy absorbing structures for barge collision protection of bridge piers" (2013).
- [4] Yanyan Sha and Hong Hao, "Nonlinear finite element analysis of barge collision with a single bridge pier" (2012).
- [5] Zhenhui Liu, "Analytical and numerical analysis of iceberg collision with ship structures", Department of Marine Engineering, University of Science and Technology (2011).
- [6] S Zhang, H Ocakli and P T Pedersen, "Crushing of ship bows in head on collision", International Journal of Maritime Engineering (2004).
- [7] Sabarethinam Kameshwar, Jamie E. Padgett, "Response and fragility assessment of bridge piers subjected to barge bridge collision and scour", Department of Civil and Environment Engineering, Rice University (2008).
- [8] AASHTO, Guide Specification and Commentary for Vessel Collision Design of Highway Bridge, GVCB-1. American Association of State Highway and Transportation Officials, Washington, DC (1991).
- [9] D. Moulas, M. Shafiee, A. Mehmanparast, "Damage analysis of ship collisions with offshore wind turbine foundations" (2017).
- [10] Kim J, Kang SJ, Kang BS, "A comparative study of implicit and explicit FEM for the wrinkling prediction in the hydroforming process" Int. J. Adv. Manuf. Technol. (2003).